ISSN: 0067-2904

The Relationships between Supermassive Black Holes and Star Formation Rate in Active Galaxies using Optical Spectra Variability

Narjes Abd Al_rhman Japar, Y. E. Rashed
Department of Astronomy and Space, Collage of Science, University of Baghdad, Baghdad, Iraq

Received: 2/1/2024 Accepted: 28/4/2024 Published: 30/4/2025

Abstract

The purpose of this research is to examine the variation in star formation rate for two types of active galaxy models. It also aims to study the relationship between supermassive black holes (SMBH) and the star formation rate (SFR) for 29 samples of active galaxies. These objects have been classified into two types: 19 samples of the Quasar and 10 samples of the Seyferts. These galaxies have been selected from the Sloan Digital Sky Survey (SDSS), at different time intervals, and they have been monitored twice or more times during a period of approximately 10 years. The results in this article show that the value of the standard deviation star formation rate variability with respect to SMBH in QSO is higher than the standard deviation star formation rate variability with respect to SMBH in Seyferts as present, respectively (19.5 and 16.8). Moreover, a good linear correlation has been found between the SMBH and the SFR within the Seyfert and QSO galaxies, exhibiting varying degrees of goodness. This correlation is attributed to the clear impact of the bright active galactic nuclei characteristics among these objects. Additionally, the variability of the emission-lines ([O_{II}], [H_β], [O_{III}], [H_α], [S_{II}]) has been studied for both samples (QSO and Seyferts), and it has been found that (([H_β], [O_{II}], [S_{II}]) are highly affected by the gravitational bound system of the central black hole of the hosting galaxy. Furthermore, it has been noticed that bulge host mass (M_{bulge}) is linearly correlated with the centrally black hole mass of the host galaxies, leading us to the direct connotation between these parts. On the other hand, no obvious relationship was found between the luminosities at the V-band with respect to the SFR.

Keywords: Active Galaxies, Seyfert, Quasar, Variability, Spectra.

العلاقات بين الثقوب السوداء هائلة الكتلة ومعدل تكوين النجوم في المجرات النشطة باستخدام تقلب الأطياف البصرية

نرجس عبدالرحمن جبار , ياسرعزالدين رشيد
قسم الفلك والفضاء، كلية العلوم، جامعة بغداد، بغداد، العراق

الخلاصة

الغرض من هذا البحث هو دراسة التباين في معدلات تكوين النجوم لنوعين من نماذج المجرات النشطة. بالإضافة إلى دراسة العلاقة بين الثقوب السوداء فائقة الكتلة (SMBH) ومعدل تكوين النجوم (SFR) لـ 29 عينة من المجرات النشطة. تم تصنيف هذه الأجسام إلى أنواع: 19 عينة من الكوازار و10 عينات من سيفرت. تم اختيار هذه المجرات من Sloan Digital Sky Survey (SDSS)، وتم رصدها على فترات زمنية مختلفة

*Email: nrjs220@gmail.com

مرتين إلى أكثر خلال فترة زمنية تبلغ حوالي 10 سنوات. توضح النتائج في هذه المقالة أن قيمة تقلب معدل تكوين النجوم بالانحراف المعياري فيما يتعلق بـ SMBH في QSO أعلى من تقلب معدل تكوين النجوم بالانحراف المعياري فيما يتعلق بـ SMBH في Seyferts كما هو موجود على التوالي (19.5 و16.8). علاوة على ذلك، تم العثور على علاقة خطية جيدة بين SMBH وSFR داخل مجرتي سيفرت وQSO، مما يظهر درجات متفاوتة من الجودة. ويعزى هذا الارتباط إلى التأثير الواضح لخصائص النوى المجرية النشطة الساطعة بين هذه الأجسام. بالإضافة إلى ذلك، تمت دراسة تباين خطوط الانبعاث ([O_{II}]، [H_β]، [O_{III}]، [H_α]، [S_{II}]) لكلا العينتين (QSO وSeyferts) ووجد أن ([H_β]، [O_{II}]،[S_{II}]) تتأثر بشدة بنظام الجاذبية للثقب الأسود المركزي للمجرة المضيفة. علاوة على ذلك، فقد لوحظ أن كتلة الانتفاخ المركزي للمضيف (M_{bulge}) ترتبط خطيًا بكتلة الثقب الأسود المركزي البالغة للمجرات المضيفة، وهذا يقودنا إلى الدلالة المباشرة بين هذه الأجزاء، ومن ناحية أخرى، لم يتم العثور على علاقة واضحة بين اللمعان في النطاق V بالنسبة إلى SFR.

1. Introduction

Compared to other types of galaxies, active galaxies produce more energy and light in their stars. They are distinguished by a few characteristics that are absent from typical galaxies, like great luminosity, spectrum emission variability, and nonthermal radiation [1]. They are mostly laying at high redshift; in addition, the active galactic nuclei (AGN) are 100 times brighter than the host galaxy [2] [3] [4]. One of the most significant sources of energy for active galaxies is the supermassive black hole (SMBH), which is located in the galaxy's center and prevents any light sources from escaping due to its high gravity [5]. Active galaxies, which are propelled by the accretion of matter onto supermassive black holes at their centers, frequently exhibit variability, from radio waves to gamma rays. The variability in active galaxies happens throughout a wide spectrum of wavelengths, and it offers important new information on the physical processes taking place both close to the central black hole and in the surrounding space [6]. These active objects exhibit several primary categories of variability: intraday variability, short-term variability, long-term variability, and flux variability [7].

Active galaxies show a very clear variation at different wavelengths (such as radio, x-ray, and optical) [8] . This discrepancy has several reasons, including the instability of the galaxy disk, a defect in the micro lens, the starburst that occurs inside the galaxy, and others. This discrepancy is detected by observing active galaxies for different periods of time [9].

Galaxies can show variations in their star formation rate (SFR) over a range of periods, from millions to billions of years. Numerous elements, including interactions with nearby galaxies, gas accretion, and internal galactic dynamics, can have an impact on this variation.

In 1981, the fluctuation of the absolute energy distribution and emission lines of the following galaxies: 3C 382 and 3C 390.3 was investigated by H. K. C. Yee and J. B. Oke using multichannel spectrophotometric data gathered from 1969 to 1980. They found that the data were consistent with the hypothesis that the variation in continuity was due to a nuclear variable component superimposed on an elliptical galaxy component [10]. In 2017, John J. Ruan, used SDSS repeat spectroscopy to comprehend the development of apparent AGN anisotropy phenomena in ultraviolet/optical light. Many repetition spectra in this data set cover a time period of more than ten years. Recent spectroscopic and imaging studies indicate that nearly all Type I quasars are optically variable [11].

Dataset

A 2.5-meter wide-angle optical telescope called the Sloan Digital Sky Survey (SDSS) is devoted to the Apache Point Observatory in New Mexico. The project, which bears the founder's name and was supported by Alfred P. Sloan, started in 2000.Simply put, the Sloan

Digital Sky Survey is the most ambitious astronomical survey ever undertaken. The survey maps one-quarter of the entire sky in detail (25% of the celestial sphere), approximately 10,000° centered on the north galactic polar. It determines the positions and absolute brightness of hundreds of millions of celestial objects. It also measures distances to more than a million galaxies and quasars [12] .

1.1 Data Collection

In this paper, the focus was on the two most important types of active galaxies, where data were collected for 19 quasars and 10 Seyferts, which were collected from the Sloan Digital Sky Survey (SDSS) website, 16th edition, as listed in Tables (1 and 2). The largest astronomical survey that has ever been conducted was the (SDSS). Using detailed maps of one-fourth of the sky, the survey pinpoints the locations and absolute brightness of hundreds of millions of celestial objects. More than tens of thousands of galaxies and quasars' distances were also measured [13]. It gathered deep, multi-color photos during the course of its eight-year operations (SDSS-I, 2000–2005; SDSS–II, 2005–2008) and produced 3-dimensional maps of more than 930,000 galaxies and more than 120,000 quasars. There are more than 30,000 pairs of repeat quasar spectra in the SDSS spectroscopic library, encompassing a wide range of time-lags up to more than 10 years in the rest-frame [12]. Using the sixteen data releases of the SDSS survey, this research employed SDSS for active galaxies (Quasar and Seyfert) with repeated spectra to examine various characteristics of active galactic nuclei.

1.2 Data reduction

The direct measurement of physical parameters associated with SDSS optical spectra necessitates a multi-stage data processing approach, specifically data reduction. The raw spectra from quasars contain components like the stellar continuum, Fe_{II} emission lines, and a dominating power-law structure, all of which need to be subtracted. To effectuate these corrections, a Python-based pipeline, originally developed by [14], was adapted and employed for sample fitting in this project. This pipeline facilitated the computation of key physical information, including flux density (fv), full width at half maximum (FWHM), dispersion velocity (σ), and the identification of emission lines. As previously mentioned, modifications were made to this code to tailor it to QSO spectra, involving distinct stages outlined in Figures 1 and 2, respectively. These stages are succinctly described as follows:

1. Subtract the stellar continuum.
2. Subtract the [Fe_{II}] emission lines [15].
3. Fit the power-law template and normalize the spectrum to the zero-level, enabling the measurement of the intensity of the required emission lines and the determination of FWHM.

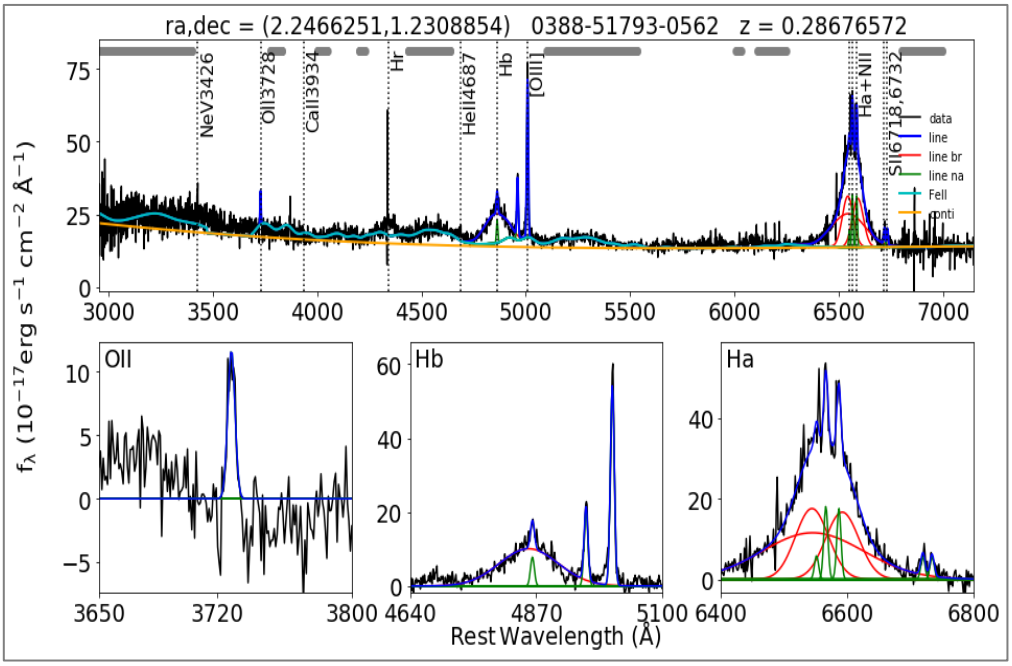

Figure 1: Spectral modeling of QSO. The observed quasar is present in a black line. Staller-continuum is present in a fain brown line. The fitting profiles are shown in various colors.

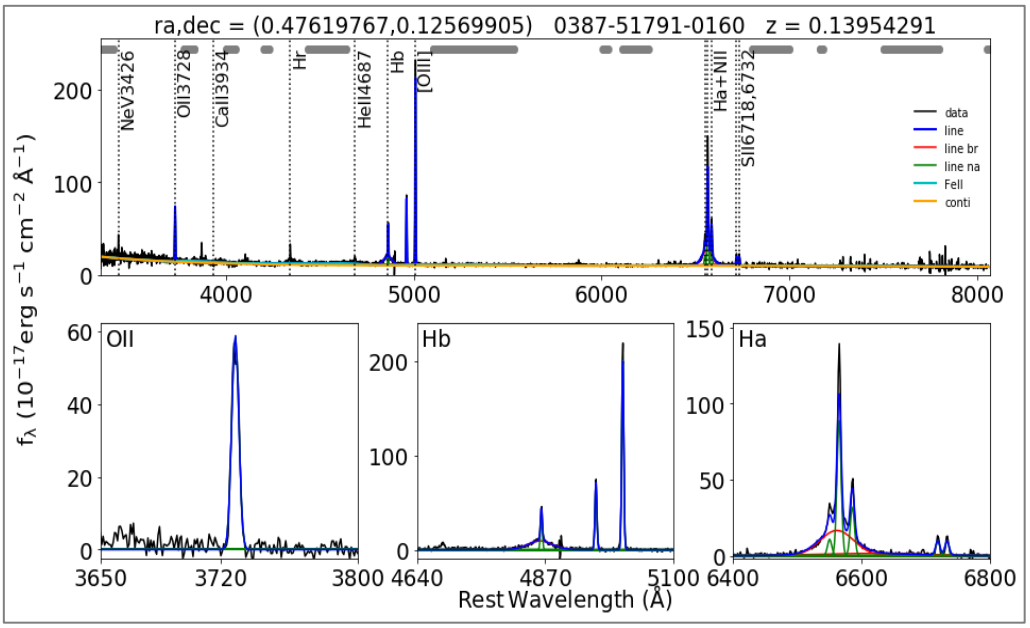

Figure 2: Spectral modeling for Seyfert galaxies. The observed galaxy is shown in a black line. The staller continuum is present in a faint brown line. The fitting profiles are in different colors.

2. The Mathematical Model to Calculate the Supermassive Black Holes and the Star Formation Rate

To understand the origin, formation, and evolution of galaxies, it's necessary to study the correlation between the physical properties of hosting galaxies. One of these parameters are the relationships between supermassive black holes and the rate of star formation. A mathematical model has been taken from recent studies. To understand the behavior of the host galaxy, these calculations use many factors, such as the gas density and the mass of the central black hole surrounding the gravitational system. Through the results and calculations, it is possible to obtain an understanding of the physical processes that govern the evolution of

black holes and the formation of stars. This research explains the basic processes in the formation of the universe because it's having a major impact on astrophysics. In this section, the mathematical equations that were used to calculate SMBH and SFR will be presented.

3.1 Calculation of the Supermassive Black Hole

A supermassive black hole is a particular type of black hole with a mass up to millions or even billions of times greater than the Sun mass (M_{sun}). The expression "black hole" refers to the area that has extremely strong gravitational force, mainly lying at the center of a galaxy, such as our galaxy (the Milky Way), and from which nothing, not even light, can get-away. Various processes, such as the collapse of massive gas and dust clouds onto an existing black hole, or the collision of many smaller black holes, are theorized to produce supermassive black holes. Supermassive black holes have a dramatic influence on the circumference around them because of their powerful gravitational force [16]. They have a deep impact on the dynamics and structure of the host galaxy, which includes how stars are formed and how matter is extended. Quasars and active galactic nuclei (AGN) sources release powerful radiation and jets of particles as matter collapses into the black hole's gravitational force [17]. Supermassive black holes have an important role in understanding the universe's evolution [18].
To calculate a supermassive black hole mass, the following formula was used [19] [20]: -

$$\log\frac{M_{BH}}{M_{\odot}} = 8.12 + \log\left(\frac{\sigma *}{200\ km.S^{-1}}\right)^{4.24\pm0.41} \quad \ldots\ldots\ldots\ldots\ldots\ldots (1)$$

$$\text{or} \quad \log\frac{M_{BH}}{M_{\odot}} = \log\left((2.1 * 10^{8}) * \frac{\sigma*}{200\ km.S^{-1}}\right)^{5.64} \quad \ldots\ldots\ldots\ldots (2)$$

\

$\log\frac{M_{BH}}{M_{\odot}}$: represents the central black hole mass in respect to solar mass.
σ∗: dispersion velocity.

3.2 Star Formation Rate Calculation

Star formation rate (SFR) represents the amount of the stellar mass that is created over a period of time, and measured in units of solar mass per year. Studying the process of galaxy evolution through time depends on understanding the SFR, which is the signature of stellar activity in galaxies [21]. Determining from the spectral emissions of high redshift galaxies, where stars are most highly distributed and generate the most energy, or using an astronomical observatory to locate new stellar flares, are important methods that can be used to quantify the rate of star formation [22]. A variety of variables, including temperature, pressure, intragalactic disturbances, interferences with magnetic fields, and gas and dust densities, the rate of star formation can enlarge the variations within as well as between galaxies. Knowing the rate of star formation is important to understand the evolution of galaxies and the appearance of cosmic structures throughout time in astronomy and cosmology studies [23].

To measure the star formation rate (SFR), the luminosities of [O_{II}] were used [19] [24] .

$$\text{SFR}_{[OII]}\ [M_{\odot}\ \text{yr}^{-1}] = \frac{L_{[O_{II}]}}{2.97 \times 10^{33} W} \quad \ldots\ldots\ldots\ldots\ldots\ldots (3)$$

To calculate the luminosities

$$L_{[O_{II}]} = 4\pi \times D_L \times S \quad \ldots\ldots\ldots\ldots\ldots\ldots\ldots\ldots\ldots\ldots (4)$$

Where D_L: luminosity distance in units (Mpc), S: flux density for each [O_{II}] line in units (erg. cm^{-2}. s^{-1}**)**.

The luminosity distance D_L has been calculated for each galaxy by combining the redshift with the cosmological constants H_o = 70 (km s^{-1} Mpc^{-1}), Ω_m = 0.3(OmegaM), and Ω_Λ = 0.7(Omegavac) [25] [24].

To measure the mass of the bulge (M_{Bulge}), we use this equation [26]:-

$$\frac{M_{BH}}{M_\odot} = 2.9 \times 10^8 \left(\frac{M_{bulge}}{10^{11}\, M_\odot}\right)^{1.05} \quad \ldots\ldots\ldots\ldots\ldots\ldots (5)$$

$\frac{M_{bulge}}{M_\odot}$: represents the mass of the bulge with respect to the mass of the sun.

While measuring luminosities in the V-band, we use this equation (equation of absolute magnitude) [27]:-

$$M_V - M_{V\odot} = -2.5 \log \frac{L_V}{L_{VM_\odot}} \quad \ldots\ldots\ldots\ldots\ldots\ldots (6)$$

$$\frac{L_V}{L_{VM_\odot}} = 10^{-0.4(M_V - M_{V\odot})} \quad \ldots\ldots\ldots\ldots\ldots\ldots\ldots (7)$$

$\frac{L_V}{L_{VM_\odot}}$: represents the luminosities of the quasars in the V-band with respect to the luminosity of the sun in the same band, M_V: absolute magnitude at the V-band.

3. Results and Discussions

These data have been randomly selected from the SDSS survey. The results of this project showed the relationship between supermassive black holes (SMBH) and star formation rate (SFR) for active galaxies of the Seyfert type and the Quasar type. Where Equation (2) was used to calculate the value of SMBH and Equation (3) was used to calculate the value of SFR. It has been found that the galaxies of Seyfert have a good linear correlation between SMBH and SFR, as well as Quasar; that is, in general, there seems to be a continuous trend to increase SFR with SMBH, according to Figures 3 and 4, and these results are matching with [28]. The linearity indicates a clear relationship, compared to other studies that were obtained on a large scale, due to the direct effect of the gravitational force of central black and gas cloud in the board line region (BLR) and narrow line region (NLR), where these two regions generated the emission-lines at the optical spectra [29]. Furthermore, a good relationship was observed, and it can explain that the universe contains active-luminosity galaxies with a huge black hole mass lying at the center, and it's heavier than the normal galaxies from the central mass aspect. Furthermore, the bonding force of the SMBH gravity system leads to the formation of more stars. Sometimes the connection between SMBH and SFR indicates the existence of a gaseous source that improves the activity of the central mass. However, a number of studies also point to something else where active nuclei can promote or suppress star formation due to feedback processes [30].

To point out the difference between the two types of active galaxies in their line variability, we calculated the median as well as the standard deviation, as shown in Figures 5 and 6, where they represent the correlation between the SMBH and variability SFR. It has been found that the median of the Seyfert type is slightly higher than that of the QSO type, due to the reason that the Seyfert galaxies are distinguished by their higher energy.

Table 1: Data of Quasar galaxies, showing the coordinates, observing parameters, redshifts, dispersion velocity, flux density, and the value of SMBH and SFR [31] [32].

No.	Name	Coordinate		Observed data Y M D	Redshift (z)	D_L [Mpc]	σ [OIII] (km/s)	Flux density of [OII] [10^{-17}erg. cm^{-2}. s^{-1}]	$log \frac{M}{M}$.	Average $log \frac{M}{M}$	SFR [OII] [$M_\odot$ yr^{-1}]	Average SFR
		RA h mm ss	DE ° ′ ″									
1	SDSS_J000859.18+011351.1	00 08 59.18	01 13 51.1	2000 9 5	0.287	1391.5	215.6	60.1	8.5	8.45	4.68	3.74
				2017 10 14			209.5	36	8.4		2.80	
2	SDSS_J015530.02-085704.0	01 55 30.02	-08 57 04.0	2001 9 15	0.165	791.8	139.05	410.3	7.4	7.45	10.3	9.37
				2013 12 2			146.06	335.1	7.5		8.4	
3	SDSS_J093257.71+475249.4	09 32 57.71	+47 52 49.4	2002 2 10	0.198	969.1	235.6	189.9	8.7	8.65	7.18	6.18
				2014 3 3			227.3	137.3	8.6		5.19	
4	SDSS_J103427.38+614820.3	10 34 27.38	61 48 20.3	2002 4 10	0.164	786.5	245.9	177.4	8.8	8.73	4.41	4.7
				2002 4 11			246.0	188.7	8.8		4.70	
				2014 1 1			233.2	201.3	8.6		5.01	
5	SDSS_J110436.33+212417.8	11 04 36.33	21 24 17.8	2007 2 17	0.188	914.8	162.6	275.4	7.8	7.85	9.28	7.13
				2012 12 17			172.1	148.1	7.9		4.99	
6	SDSS_J113617.11+441022.5	11 36 17.11	44 10 22.5	2004 3 18	0.198	969.1	137.9	192.7	7.4	7.7	7.28	6.52
				2013 4 3			171.06	161.2	7.9		6.09	
				2013 4 6			164.3	167.5	7.8		6.33	
				2016 12 9			158.3	169.1	7.7		6.39	
7	SDSS_J122325.74+453803.7	12 23 25.74	45 38 03.7	2003 6 30	0.199	974.6	271.8	151.0	9.0	9.06	5.77	5.88
				2013 3 18			285.9	140.7	9.1		5.38	
				2014 4 29			276.2	170.4	9.1		6.51	
8	SDSS_J135852.46+295413.1	13 58 52.46	29 54 13.1	2006 4 28	0.114	529.6	154.9	101.2	7.6	7.75	1.14	1.1
				2013 2 15			174.8	94.3	7.9		1.06	
9	SDSS J081425.89+294115.6	08 14 25.89	29 41 15.6	2002 12 9	0.374	1197.4	153.7	64.2	7.6	7.76	3.70	3.38
				2010 12 11			167.1	54.2	7.8		3.12	
				2018 1 14			171.7	57.5	7.9		3.32	
10	SDSS_J110051.02+513502.1	11 00 51.02	51 35 02.1	2002 3 19	0.214	1057.2	215.3	65.1	8.5	8.43	2.93	2.22
				2013 4 2			203.94	23.0	8.3		1.03	

				2015 4 14			217.1	60.6	8.5		2.72	
11	SDSS_J110540.09+064225.6	11 05 40.09	06 42 25.6	2003 3 24	0.231	1152.2	173.7	219.2	7.9	7.9	11.71	11.41
				2011 12 30			169.2	208.1	7.9		11.12	
12	SDSS_J000512.52-000206.8	00 05 12.52	-00 02 06.8	2002 9 9	0.304	1483.1	199.6	15	8.3	7.95	1.32	2.03
				2002 10 11			167.4	27.2	7.8		2.40	
				2001 10 20			167	23	7.8		2.03	
				2002 9 1			174.6	26.9	7.9		2.38	
13	SDSS_J081501.85+525255.5	08 15 01.85	+52 52 55.5	2004 10 18	0.125	584.9	177	186.1	8	8	2.56	2.7
				2014 3 29			177.4	206.2	8		2.84	
14	SDSS_J090022.27+503138.1	09 00 22.27	+50 31 38.1	2001 3 23	0.148	702.8	128.3	25.04	7.2	7.25	0.49	0.3
				2014 3 28			140.7	6.5	7.4		0.12	
15	SDSS_J110537.62+585120.7	11 05 37.62	58 51 20.7	2002 4 13	0.191	931.0	287.44	361.7	9.2	9.3	12.62	10.68
				2014 1 8			312.1	257.4	9.4		8.98	
				2016 1 7			301.1	299.32	9.3		10.44	
16	SDSS_J081032.72+565105.2	08 10 32.72	56 51 05.2	2005 1 15	0.276	1410.8	163.6	43.0	7.8	7.75	3.44	2.67
				2014 2 20			158.9	23.8	7.7		1.90	
17	SDSS J081249.58+463050.7	08 12 49.58	46 30 50.7	2000 12 5	0.282	1410.8	284.6	15.1	9.1	9.13	1.21	1.21
				2000 11 19			263.4	19.6	8.9		1.57	
				2014 2 24			311.2	10.7	9.4		0.85	
18	SDSS J101931.79+262643.2	10 19 31.79	26 26 43.2	2006 1 29	0.250	1260.2	247.28	331.9	8.8	8.76	21.22	18.96
				2012 12 17			246.5	293.1	8.8		18.74	
				2017 5 1			236.4	265.0	8.7		16.94	
19	SDSS_J103421.71+605318.1	10 34 21.71	60 53 18.1	2002 1 21	0.228	1135.3	226.9	76.4	8.6	8.5	3.96	4.34
				2014 1 1			209.6	91.2	8.4		4.73	

Table 2: Data of Seyfert galaxies, showing the coordinates, observing parameters, redshifts, dispersion velocity, flux density, and the value of SMBH and SFR [31] [32].

No.	Name	Coordinate		Observed data Y M D	Red shift (z)	D_L [Mpc]	σ [O_{III}] (km/s)	Flux density of [O_{II}] [10^{-17}erg. cm^{-2}. s^{-1}]	$log\frac{M}{M_\odot}$.	Average $log\frac{M}{M_\odot}$	SFR [OII] [$M_\odot$ yr^{-1}]	Average SFR
		RA h mm ss	DE ° ′ ″									
1	SDSS_J000154.27+000732.4	00 01 54.27	00 07 32.4	2000 9 3	0.140	641	103.7	292.8	6.7	6.6	4.84	4.48
				2001 10 20			97.4	249.2	6.5		4.12	
2	SDSS_J000000.47-002703.9	00 00 00.47	-00 27 03.9	2001 10 20	0.250	1195.5	109.6	19.1	6.8	6.85	1.09	1.31
				2010 10 7			112.9	26.7	6.9		1.53	
3	SDSS_J083045.40+450235.8	08 30 45.40	+45 02 35.8	2001 3 17	0.182	882.4	132.9	124.6	7.3	7.5	3.90	3.18
				2014 2 28			155.3	78.8	7.7		2.47	
4	SDSS_J103942.29+230102.8	10 39 42.29	23 01 02.8	2006 11 18	0.166	797.1	190.2	500.9	8.1	8.35	12.81	13.05
				2009 2 20			195.3	520.1	8.2		13.30	
				2013 2 10			216.5	524.5	8.5		13.42	
				2018 1 23			225.8	496.4	8.6		12.70	
5	SDSS_J080037.62+461257.9	08 00 37.62	46 12 57.9	2000 12 5	0.239	1197.4	316.3	138.9	9.4	9.35	8.02	7.78
				2014 2 24			300.2	130.7	9.3		7.54	
6	SDSS_J105220.30+454322.2	10 52 20.30	45 43 22.2	2004 2 17	0.240	1203.1	197.0	87.1	8.2	8.2	5.07	4.28
				2014 5 3			196.0	59.9	8.2		3.49	
7	SDSS_J102314.55+240742.6	10 23 14.55	+24 07 42.6	2005 12 29	0.189	920.2	222.5	214.6	8.5	8.55	7.31	6.25
				2013 1 16			227.5	152.5	8.6		5.20	
8	SDSS_J115845.43-002715.7	11 58 45.43	-00 27 15.7	2000 4 28	0.095	438.8	82.05	69.1	6.1	6.1	0.5	0.45
				2001 1 20			81.7	52.5	6.1		0.4	
9	SDSS J022414.66+002415.5	02 24 14.66	00 24 15.5	2001 10 22	0.383	2063.8	255.2	8.8	8.9	8.72	1.5	2.68
				2012 11 6			205.6	15.7	8.3		2.6	
				2012 12 6			239.01	22.0	8.7		3.7	
				2013 10 11			259.4	19.0	8.9		3.2	
				2013 11 8			245.7	14.4	8.8		2.4	
10	SDSSJ000021.11-023536.1	00 00 21.11	-02 35 36.1	2011 9 5	0.454	2524.1	235.3	10.0	8.7	8.65	2.5	2.5
				2016 11 20			228.5	10.0	8.6		2.5	

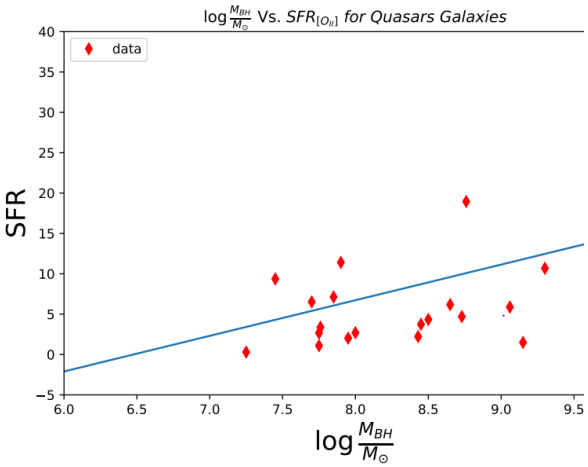

Figure 3: The correlation between the SMBH & SFR for Quasar galaxy.

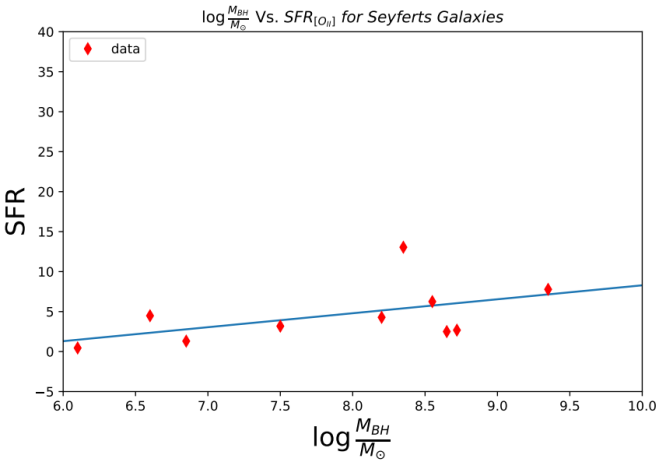

Figure 4: The correlation between SMBH & SFR for Seyfert galaxy.

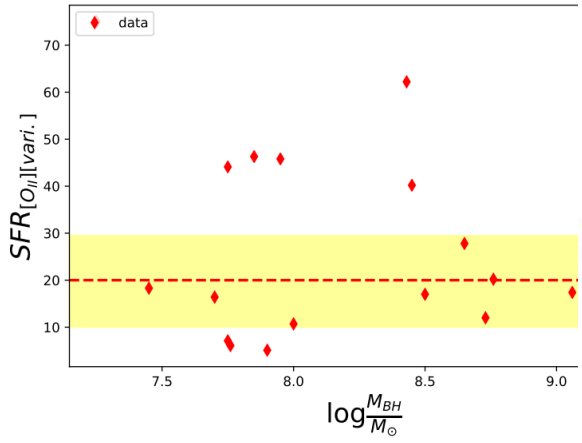

Figure 5: The correlation between the SMBH & variability SFR for Quasar galaxy. In addition, the median value is equal to 20 and the standard deviation equal to19.5.

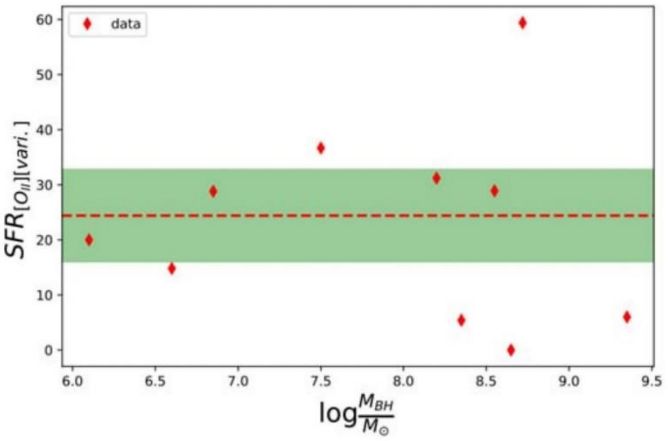

Figure 6: The correlation between the SMBH & variability SFR for Seyfert galaxy. In addition, is the median value is equal to 24.4 and the standard deviation is equal to 16.8.

The word "bulge" in the context of galaxies describes a center concentration of stars that differs from the galaxy's expansive disk and is usually spherical or elliptical. One of the most important factors influencing the galaxy's general mass distribution and dynamics is the bulge's mass. Variability in luminosity is a key characteristic that sets active galaxies apart from typical, dormant galaxies.

In order to determine the mass of the galactic bulge (M_{bulge}), equation (5) was used with respect to central black hole mass, while the V-band luminosity was derived from formula (7) (see Tables 3 and 4). Figures 7 and 8 reveal a distinct evolutionary trend in the relationship between the supermassive black hole (SMBH) and the bulge for both Quasars and Seyferts. These figures utilize equation (5) to explore the growth of SMBHs and bulges within host galaxies, which showed a good relationship between them because the relative growth of bulges and black holes from the existing cold gas supply present during the merger is roughly constant over time [33]. Figures 9 and 10 show no significant evolution in the V-band luminosity (Lv) for either Quasars or Seyferts in relation to star formation rate (SFR), despite employing Equation (7) for Lv calculations [34] [35].

Table 3: The physical measurements for Quasar (absolute magnitude in V-band, luminosity at V-band, and bulge mass)

No.	Name	Mv [Mag]	$\log\frac{M_{Bulge}}{M_{\odot}}$	$\frac{L_V}{L_{VM_{\odot}}}$
1	SDSS_J000859.18+011351.1	18.81	2.93	5.56
2	SDSS_J015530.02-085704.0	17.02	2.5	4.75
3	SDSS_J093257.71+475249.4	18.41	3	5.2
4	SDSS_J103427.38+614820.3	18.17	3.3	5.2
5	SDSS_J110436.33+212417.8	17.38	2.6	4.89
6	SDSS_J113617.11+441022.5	18.11	2.5	5.17
7	SDSS_J122325.74+453803.7	18.8	3.1	5.4
8	SDSS J135852.46+295413.1	17.7	2.62	5.01
9	SDSS J081425.89+294115.6	18.56	2.62	5.35
10	SDSS J110051.02+513502.1	18.31	2.93	5.25
11	SDSS J110540.09+064225.6	17.94	2.72	5.11
12	SDSS_J000512.52-000206.8	19.35	2.86	5.66
13	SDSS_J081501.85+525255.5	17.02	2.75	4.75
14	SDSS_J090022.27+503138.1	17.75	2.48	5.03
15	SDSS_J110537.62+585120.7	17.04	3.17	4.76
16	SDSS J081032.72+565105.2	19.36	2.68	5.66
17	SDSS J081249.58+463050.7	18.49	3.13	5.32
18	SDSS J101931.79+262643.2	18.67	3.03	5.39
19	SDSS J103421.71+605318.1	17.72	2.96	5.02

Table 4: The physical measurements for Seyfert (absolute magnitude in V-band, luminosity at V-band, and bulge mass)

No.	Name	Mv [Mag]	$\log\frac{M_{Bulge}}{M_{\odot}}$	$\frac{L_V}{L_{VM_{\odot}}}$
1	SDSS_J000154.27 +000732.4	19.48	2.31	5.71
2	SDSS_J000000.47-002703.9	20.09	2.34	5.95
3	SDSS_J083045.40+450235.8	18.02	2.51	5.14
4	SDSS_J103942.29+230102.8	18.20	2.79	5.21
5	SDSS J080037.62+461257.9	18.32	3.24	5.26
6	SDSS J105220.30+454322.2	19.11	2.82	5.56
7	SDSS_J102314.55+240742.6	17.71	2.93	5.02
8	SDSS_J115845.43-002715.7	____	2.1	0
9	SDSS J022414.66+002415.5	19.84	3.06	5.85
10	SDSS J000021.11-023536.1	____	3	0

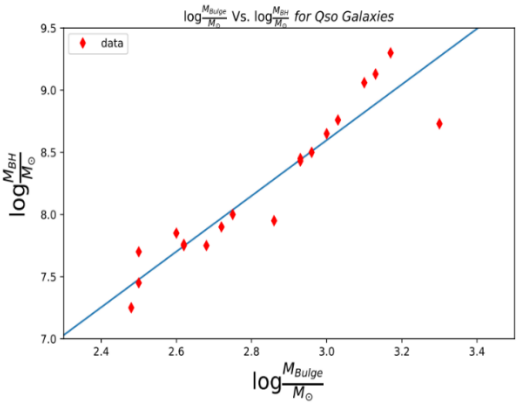

Figure 7: Shows the relation between central black hole bulge host mass (M_{bulge}) for Quasar.

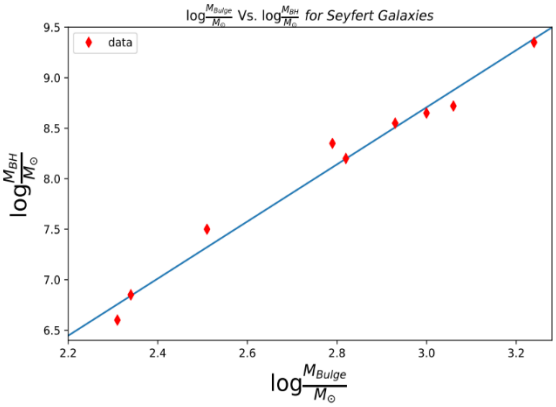

Figure 8: Shows the relation between central black hole mass and bulge host mass (M_{bulge}) for Seyfert galaxy**.**

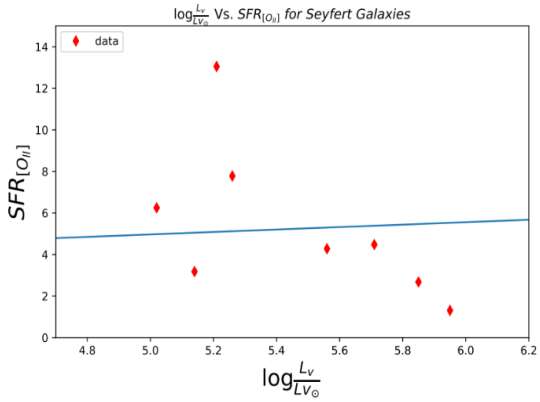

Figure 9: The relation between Quasar luminosities at V-band with respect to the luminosity of the sun same the SFR

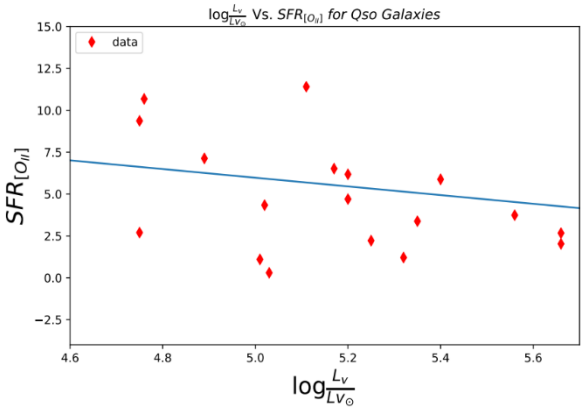

Figure 10: The relation between Seyfert galaxy luminosities at V-band with respect to the luminosity in the band and the SFR of the sun in the same band and.

The dispersion velocity of the [O_{III}] gas refers to the velocity dispersion of ionized oxygen atoms emitting [O_{III}] spectral lines within a region, typically observed in emission nebulae or the interstellar medium (ISM) of galaxies. According to Figures 11 and 12, it has been found that there is a good linear correlation between the central supermassive black hole masses and the dispersion velocity of the [O_{III}] gas for Quasar and Seyfert galaxies, and that means that there is a clear effect by increasing the SMBH masses with respect to the dispersion velocity of the [O_{III}] gas due to the force gravitational bound system of SMBH. The relation of normal galaxies exhibits far less scatter than active galaxies [36].

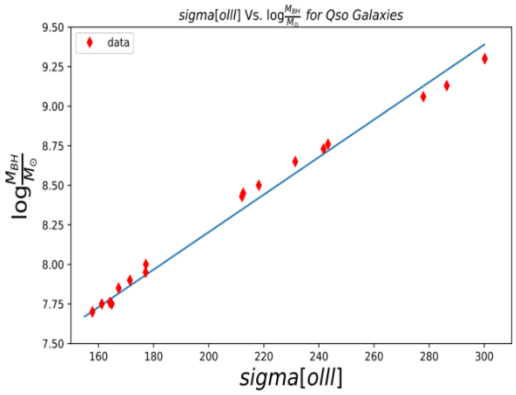

Figure 11: Shows the correlation between dispersion velocities and the central black hole masses of Seyfert.

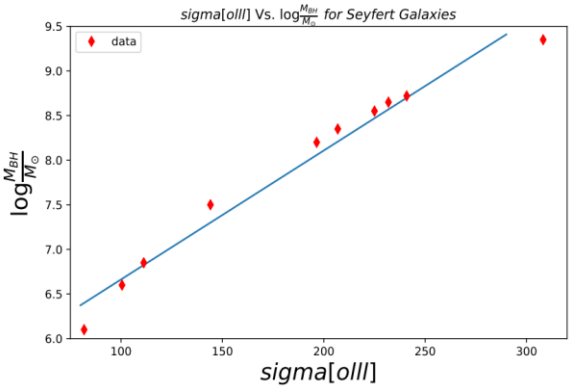

Figure 12: Shows the correlation between dispersion velocities and the central black hole masses of Quasar.

The intense activity in the central regions of active galaxies is apparent in many ways, one of these fundamental characteristics is emission-line variability. The study showed the contrast of the emission lines ([O_{II}], [H_β], [O_{III}], [H_α], and [S_{II}]) as presented in Tables (5 and 6), which were using Python programming, for both samples (Quasar and Seyferts). The most abundant elements in both types of Quasars and Seyfert were determined by calculating the median and standard deviation of all emission lines, as shown in Figures 13 and 14. Analysis of optical emission lines across a sample of Quasars and Seyfert galaxies revealed distinct variability patterns. Median luminosity values for [O_{II}] and [H_α] were significantly higher in Quasars (27.7 and 22.8, respectively) compared to Seyferts (17.5 and 19.2). Conversely, Seyferts exhibited higher median luminosities for [H_α] and [S_{II}] (24.8 and 22.4) compared to Quasars (22.6 and 20.3). This suggests that narrow-band emission lines (e.g., [O_{II}], [S_{II}]) display greater relative variability compared to broad-band lines (e.g., [H_α]) in active galactic nuclei (AGNs). This finding aligns with previous observations suggesting that narrow-band lines were more sensitive to changes in the accretion disk or central engine activity [37] [38] .

Table 5: Data of Quasar galaxies, showing the variability percentage in the emission lines.

No.	Name	Vair (O_{II})	Vair (O_{III})	Vair (H_α)	Vair (H_β)	Vair (S_{II})
1	SDSS_J000859.18+011351.1	40.1	3	25.4	1.8	20.9
2	SDSS_J015530.02-085704.0	18.4	1.7	10.2	11.8	12.7
3	SDSS_J093257.71+475249.4	27.7	3.4	31.7	41.8	8.2
4	SDSS_J103427.38+614820.3	11.9	37.6	22	14.8	63.4
5	SDSS_J110436.33+212417.8	46.23	12	4.4	6.7	45.5
6	SDSS_J113617.11+441022.5	16.4	13.3	36.3	31.2	30.1
7	SDSS_J122325.74+453803.7	17.5	13.8	35.5	43.3	22.3
8	SDSS_J135852.46+295413.1	6.9	20.3	29.7	47.3	17.6
9	SDSS J081425.89+294115.6	15.6	5.1	48.9	46	99.7
10	SDSS_J110051.02+513502.1	64.7	40.1	38.3	45.2	51.6
11	SDSS_J110540.09+064225.6	28.6	2.2	1.5	12.1	7.4
12	SDSS_J000512.52-000206.8	44.8	25.3	45.9	25.2	0
13	SDSS_J081501.85+525255.5	9.7	5.5	2.7	10.7	0
14	SDSS_J090022.27+503138.1	74	4.2	11.4	13.5	0
15	SDSS_J110537.62+585120.7	28.8	3.5	17.2	16.4	0
16	SDSS_J081032.72+565105.2	44.6	14.3	0.9	3.8	0
17	SDSS J081249.58+463050.7	45.4	10.2	2.07	5.8	0
18	SDSS J101931.79+262643.2	20.1	14.3	23.7	24.5	0
19	SDSS_J103421.71+605318.1	16.2	6.7	14	6.9	0
Median		27.7	10.2	22.8	14.4	22.3
Standard deviation		18.3	11	15.5	15.3	27

Table 6: Data of Seyfert galaxies, showing the variability percentage in the emission lines

No.	Name	Vair (O_{II})	Vair (O_{III})	Vair(H_α)	Vair(H_β)	Vair (S_{II})
1	SDSS_J000154.27+000732.4	14.9	10.6	33.9	26.9	19.3
2	SDSS_J000000.47-002703.9	28.5	6.4	25.7	3.8	31
3	SDSS_J083045.40+450235.8	36.8	3.5	22.9	25.5	24.2
4	SDSS_J103942.29+230102.8	0.9	9	28.6	42.4	26.9
5	SDSS_J080037.62+461257.9	6	6	8.8	13.1	9.7
6	SDSS_J105220.30+454322.2	31.3	1.1	4.2	23.9	72.9
7	SDSS_J102314.55+240742.6	29	4.5	23.9	7.7	20.6
8	SDSS_J115845.43-002715.7	24	42.6	0	0	66.4
9	SDSS J022414.66+002415.5	60	35.3	41.8	44.8	0
10	SDSS J000021.11-023536.1	0	24.9	37.1	12.9	0
Median		17.5	7.7	24.8	18.5	22.4
Standard deviation		26.2	13.8	13.3	14.5	27

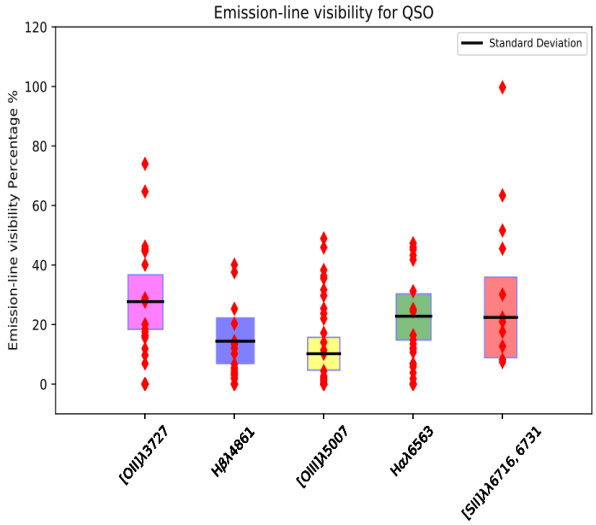

Figure 13: The variability percentage in the emission lines for Quasar.

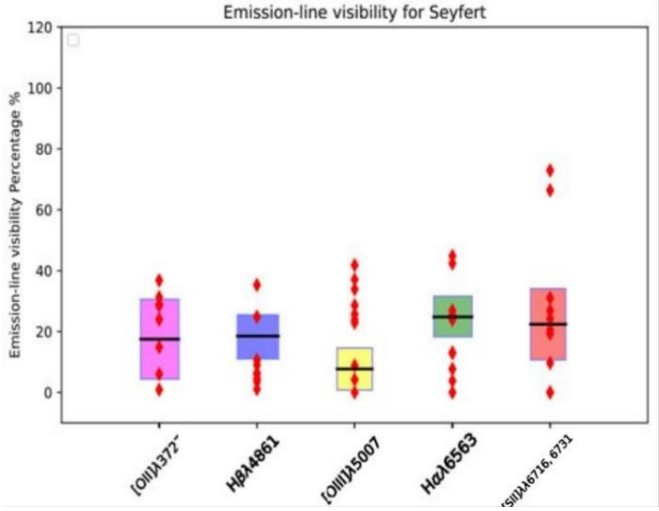

Figure 14: The variability percentage in the emission lines for Seyfert.

Conclusions:

The active galaxies, that have been examined in this research (Quasar and Seyfert galaxies), are characterized by broad emission lines and these lines are generated mainly in an area (BLR), where this area is almost located at 10^{11} km from the center of the galaxy and the speed of the cloud in this region is 5000 km. S^{-1}. This means that these lines are exposed to a direct influence from the high gravitational force generated by supermassive black holes, which prompted us to study the changes in the optical spectrum emitted by them. To be more specific, this research focused on the change in the star formation rate calculated based on the emission line (O_{II}) for supermassive black holes.

According to the previous explanation in section four, the following had been concluded:
1-The outcomes demonstrated a distinct correlation between the Seyfert's SMBH and SFR. Due to the greater influence of luminous active galactic nuclei, it is a better relationship than that of the Quasar type.

2- There is no significant evolution in the V-band luminosity (Lv) for either Quasars or Seyferts in relation to the star formation rate (SFR).
3-For Quasar and Seyfert galaxies, there is a linear relationship between the masses of the supermassive black holes in their centers and the gas's dispersion velocity. And also, there is a linear relationship between the SMBH and Mbulge.
4-Measurements were made from the emission lines that corresponded to them, the standard deviation, and the median of their relevance. According to the findings, the Seyfert emits the highest levels of [H_α] and [S_{II}], while [O_{II}] and [H_α] are the highest in the Quasar. Knowing the pace of star creation throughout time and the variance in galaxies relative to the supermassive black hole already present in each galaxy was beneficial.

References

[1] Elvis M., BRANDT W., WORRALL D., FABBIANO G., HORNSCHEMEIER A., and BRISSENDEN R., "Active Galaxies and Quasars, 2010-2020," *Astro 2010 Science white paper,* pp. 1-8, (2009).

[2] H. R. Al-baqir, A. K. Ahmed and D. Gamal, "Surface Photometry of NGC 3 Lenticular Galaxy," *Iraqi Journal of Science,* vol. 60, no. 9, pp. 2080-2086, 2019.

[3] Peterson, and B. M, "An introduction to active galactic nuclei", landan: Cambridge University Press, (1997).

[4] Z. Adnan and A. K. Ahmed, "Surface Photometry of Spiral Galaxy NGC 5005 and Elliptical Galaxy NGC 4278," *Baghdad Science Journal,* vol. 15, no. 3, 2018.

[5] Y. E. Rashed, "The relation between variable active galactic nuclei, their immediate environments, and the conditions for star formation," *Universitat zu Koln,* p. 31, 26 October 2015.

[6] S. Kozłowski, "Optical Variability of Active Galactic Nuclei," *Frontiers in Astronomy and Space Sciences,,* vol. 4, no. 14, 2017.

[7] Ulrich, M. H., Maraschi, L. and C. M. Urry, " Variability of active galactic nuclei," *Annual Review of Astronomy and Astrophysics,* vol. 35, p. 58, 1997.

[8] Y. E. Rashed, M. N. A. Najm and H. A. Dahlaki, "Studying the Flux Density of Bright Active Galaxies at Different Spectral Bands," *Baghdad Science Journal,* vol. 16, no. 1, p. 7, 2019.

[9] M. R. S. Hawkins, "Variability in active galactic nuclei: confrontation of models with observations.," *Monthly Notices of the Royal Astronomical Society,* vol. 1, no. 329, pp. 76-86, 2002.

[10] H. K. C., Oke. J., and Yee, "Optical spectral variability of the N galaxies 3C 382 and 3C 390.3," *Astrophysical Journal,* vol. 248, no. 1, pp. 472-484, Sept. 1, 1981.

[11] J. J. Ruan, "The Astrophysics of Active Galactic Nuclei Variability," *University of Washington,* p. 182, 2017.

[12] J. E. Gunn, W. A. Siegmund, E. J. Mannery, R. E. Owen, C. L. Hull, R. F. Leger, S. I. ... and Wang , "The 2.5 m telescope of the sloan digital sky survey," *The Astronomical Journal,,* vol. 4, no. 131, p. 28, 2006.

[13] Y. E. Rashed, A. Eckart, M. Valencia-S, M. García-Marín, G. Busch, J. Zuther, H. ... and Zhou, "Line and continuum variability in active galaxies," *Monthly Notices of the Royal Astronomical Society,,* vol. 3, no. 454, p. 28, 2015.

[14] Y. Shen and e. al, "“The Sloan Digital Sky Survey Reverberation Mapping Project: Sample Characterization”," *The Astrophysical Journal Supplement Series,* vol. 241, p. 16, 2019.

[15] M. N. A. Najm, H. S. Mahdi and S. A. Abdullah, "The Exponential and Gaussian Density Profiles of HI and Fe II in the Gaseous Halo of the Milky Way," *Iraqi Journal of Science,* vol. 58, no. 4, pp. 2467-2472, 2017.

[16] J. M. Miller and C. S. Reynolds, "Black holes and their environments," *physics today,* vol. 60, no. 8, p. 42–47, 2007.

[17] M. Volonteri, M. Habouzit and M. Colpi, "The origins of massive black holes," *Nature Reviews Physics,*, vol. 11, no. 3, p. 20, 2021.

[18] M. Habouzit, R. S. Somerville, Y. Li, S. Genel, J. Aird, D. Anglés-Alcázar and M. Vogelsberger, "Supermassive black holes in cosmological simulations–II: the AGN population and predictions for upcoming X-ray missions," *Monthly Notices of the Royal Astronomical Society,* vol. 2, no. 509, p. 28, 2022.

[19] P. Schneider, Extragalactic Astronomy and Cosmology, Springer, 2014.

[20] F. M. Khan, "Dynamics and Evolution of Supermassive Black Holes in Merging Galaxies," *University of Heidelberg,* p. 156, 2011.

[21] T. D. Oswalt and W. C. Keel, Planets, Stars and Stellar Systems (Extragalactic Astronomy and Cosmology), USA: Springer, 2013.

[22] A. T. Barnes, S. N. Longmore, C. Battersby, J. Bally, J. M. D. Kruijssen, J. D. H., and D. L. Walker, "Star formation rates and efficiencies in the Galactic Centre," *Monthly Notics of the Royal Astronomical Society,* no. 469, p. 23, 2017 April 21.

[23] M. R. Krumholz and C. Federrath, "The Role of Magnetic Fields in Setting the Star Formation Rate and the Initial Mass Function," *Frontiers in Astronomy and Space Sciences,* vol. 6, no. 7, p. 28, 2019.

[24] S. Salim, R. M. Rich, S. C. and other, "UV STAR FORMATION RATES IN THE LOCAL UNIVERSE," *The Astrophysical Journal Supplement Series,* p. 267_292, 2007.

[25] S. H. Kareem and Y. E. Rashed, "Studying the Correlation between Supermassive Black Holes and Star Formation Rate for Samples of Seyfert Galaxies (Type 1 and 2)," *Iraqi Journal of Physics,* vol. 19, no. 48, pp. 52-65, 2021.

[26] A. E. Reines and M. Volonteri, "RELATIONS BETWEEN CENTRAL BLACK HOLE MASS AND TOTAL GALAXY STELLAR MASS IN THE LOCAL UNIVERSE," *The Astrophysical Journal,* vol. 2, no. 82, p. 14, 2015 November 10.

[27] Z. Eker, F. Soydugan, V. Bakış, S. Bilir and I. Steer, "A Silent Revolution in Fundamental Astrophysics," *The Astronomical Journal,* vol. 5, no. 164, p. 8, 2022.

[28] Y. E. Rashed, "The Correlation between SMBH and SFR for Quasars," *Iraqi Journal of Science,* vol. 64, no. 12, pp. 6611-6619, 2023.

[29] C.-T. J. CHEN, R. C. HICKOX, S. A. and A. POPE, "A CORRELATION BETWEEN STAR FORMATION RATE AND AVERAGE BLACK HOLE ACCRETION IN STAR FORMING GALAXIES," *THE ASTROPHYSICAL JOURNAL,* vol. I, p. 9, 5 June 2013.

[30] O. Torbaniuk, M. Paolillo, F. Carrera, S. Cavuoti, C. Vignali, G. Longo and J. Aird, "The connection between star formation and supermassive black hole activity in the local Universe," *Monthly Notices of the Royal Astronomical Society,* vol. 2, no. 506, p. 19, 2021.

[31] M.-P. Véron-Cetty and P. Véron, "A catalogue of quasars and active nuclei: 13th edition," *Astronomy and astrophysics,* vol. 10, no. 518, p. 8, 29 March 2010.

[32] I. Pâris, P. Petitjean, N. P. Ross and L. Zhu., "The Sloan Digital Sky Survey Quasar Catalog: Twelfth data release," *Astronomy and Astrophysics,* vol. 79, no. 597, p. 25, 3 August 2016.

[33] D. J. Croton, "Evolution in the black hole mass–bulge mass relation:a theoretical perspective," *Monthly Notices of the Royal Astronomical Society* , vol. 4, no. 369, p. 5, 2006.

[34] H. Winkler, "Some things change, some don't. An exploration of Seyfert galaxy luminosity changes over a generation," *proceedings of science,* p. 11, 2018.

[35] A. Lapi, F. Shankar, J. Mao, G. L. Granato, L. Silva4, G. D. Zotti and L. Danese, "Quasar Luminosity Functions from Joint Evolution of Black Holes and Host Galaxies," *The Astrophysical Journal,* vol. 650, no. 1, p. 42, 2006.

[36] D. Merritt and L. Ferrarese, "Relationship of black holes to bulges," *Astronomy and physics,* vol. 2, p. 29, 2001.

[37] R. Lin, Z.-Y. Zheng, W. Hu and S. Zhu., "On the Origin of the Strong Optical Variability of Emission-line Galaxies," *The Astrophysical Journal,* vol. 1, no. 35, p. 14, 2022 November 20.

[38] M. A. Malkan, L. D. Jensen, D. R. Rodriguez and others, "Emission Line Properties of Seyfert Galaxies in the 12μm Sample," *The Astrophysical Journal*, vol. 846, no. 102, p. 26, 2017.